Radium Sorption to Iron (hydr)oxides, Pyrite, and Montmorillonite: Implications for Radium Transport

Michael A. Chen and Benjamin D. Kocar*

Dept of Civil and Environmental Engineering,

Massachusetts Institute of Technology

*Corresponding author, kocar@mit.edu

Abstract

Radium (Ra) is a radioactive element commonly found within soils, sediments and natural waters. Elevated Ra activities arising through natural and anthropogenic processes pose a threat to groundwater resources and human health, and Ra isotope ratios are used to decipher groundwater movement, estimate submarine discharge flux, and fingerprint contamination associated with hydraulic fracturing operations. Although transport and retention of Ra within subsurface environments is known to be dominated by adsorption, particularly by metal (hydr)oxides, there is limited understanding of how Ra associates with other mineral surfaces. Here, we present results of sorption studies and surface complexation modeling of Ra to ferrihydrite, goethite, montmorillonite, and pyrite, in a low salinity groundwater solution across a range of pH values. We find that ferrihydrite and goethite are major sorbents of Ra at neutral to basic pH, but that (sodium) montmorillonite retains comparatively more Ra across a wide range of pH values (normalized to either mass or surface area), owing to interlayer ion exchange. When normalized to surface area, pyrite retains the most Ra at pH 7 and 9 of all minerals examined. The results here highlight the key role of redox- conditions and associated mineralogical alterations on Ra mobility, and provide surface complexation parameters for informing models used to predict Ra transport in soil and sedimentary systems.

Introduction

Chronic ingestion and inhalation of radioactive materials, including radium (Ra) and radon (Rd), represents an ongoing threat to human health worldwide.[1] Of these, Ra is ubiquitous in soils, aquifers, and natural waters owing to the radioactive decay of primordial ^{235}U, ^{238}U, and ^{232}Th, and often accounts for the dominant fraction of total radiation found in groundwater. All isotopes of Ra are unstable, and four (^{223}Ra, ^{224}Ra, ^{226}Ra, and ^{228}Ra) possess half-lives sufficient to persist within environmental systems and present a risk for human exposure. Moreover, ^{226}Ra (half-life of 1600 years) is the parent radionuclide of ^{222}Rn; chronic inhalation of ^{222}Rn increases risk of lung cancer. Hence, geochemical controls on Ra mobility are directly tied to the mobility and accumulation of Rn within soil-sedimentary systems.[2]

Several geochemical processes impart overarching controls on Ra within soils and aquifers. Alpha-recoil, the ejection of daughter radionuclides from soil and sedimentary minerals into adjacent porewater, is the primary process sourcing Ra to groundwater. Ongoing alpha recoil progressively elevates porewater Ra activities until hydrologic flushing removes the equilibrating solution, or Ra achieves secular equilibrium with its parent radionuclides. Most aquifer systems contain low (e.g. U, Th, <5 mg/kg) but adequate parent radionuclide and sufficiently favorable hydrological conditions to facilitate delivery of measurable Ra to solution.[3] In a recent USGS study, 3% of groundwater samples (n=1270) within 7 of 15 principal US aquifers exceeded the USEPA limit for total Ra of 0.185 Bq/L.[4] Further, high levels of Ra are often present with deeper formations, particularly shales, where low groundwater flux yield potentially hazardous activities (0.102-343 Bq/L).[5] These naturally elevated Ra bearing formations are prevalent in some parts of the US (PA, WY, TX) and abroad (Middle East, etc.).[6,7] Anthropogenic activities, including uranium mining and hydraulic fracturing, can redistribute

Ra and other constituents of naturally occurring radioactive materials (NORM), posing potential hazard to soils, surface waters, and aquifers.

While Ra transport is considered to be conservative in some groundwater systems, it nevertheless participates in geochemical reactions that may alter its subsurface distribution. In general, Ra sorption to solids, particularly mineral surfaces and organic matter, imparts the greatest chemical control on soluble Ra transport in groundwater systems, rather than precipitation (or co-precipitation)-dissolution of Ra-bearing solids.[1,8,9] Under environmental conditions, Ra is not redox active, and its solution speciation is dominated by free Ra^{2+} across a wide range of chemical conditions (e.g. pH and salinity). Weak complexes with carbonate, sulfate, and chloride are observed, but these solution species dominate at extremely acidic or basic pH values and when ligand activities exceed environmentally relevant activities.[10]

Soil and sedimentary minerals known to sorb appreciable quantities of Ra include metal (hydr)oxides and 2:1 clays with an exchangeable interlayer. However, previous data are primarily derived from Ra sorption experiments using mineralogically heterogeneous soil and sedimentary solids. This has generated a wealth of reported K_d values for Ra sorption to different soil and aquifer materials, but may be of limited use when predicting Ra mobility under different or varying geochemical conditions. Moreover, few studies have examined or considered mechanisms of Ra sorption; one study used surface complexation modeling (SCM) to examine Ra adsorption to metal (hydr)oxides, but at levels far exceeding those found in most environmental systems, and was limited to Fe (hydr)oxides (goethite and ferrihydrite). [11,12] There is also a paucity of data regarding Ra adsorption to redox-sensitive minerals found under anoxic or reducing conditions. These solids, including metal sulfides such as pyrite, may be particularly

important within soil and aquifer systems derived from shale, and also within marine sediments—including those which intercept submarine groundwater discharge.

Improved knowledge of Ra sorption to common soil and sedimentary solids is required to decipher and predict Ra mobility and total activities within natural waters, and may aid in interpreting Ra isotopic ratios used to trace sources of Ra and understand groundwater movement. The objectives of this study were to therefore: 1) examine and compare low-activity Ra adsorption to ferrihydrite, goethite, and Na-montmorilonite—minerals known or inferred to control Ra transport over a range of solution conditions found in soils and aquifers—and pyrite, a mineral commonly found within reduced and anoxic soils and sediments, and 2) use SCM to constrain Ra adsorption mechanisms and provide a quantitative basis for comparing Ra adsorption to different minerals, across a range of pH values. We illustrate that Ra adsorption to montmorillonite is more extensive over a range of solution conditions compared to iron (hydr)oxides, which are often thought as dominant Ra sorbents. Further, we find that under neutral or high pH, Na-montmorillonite retains the most Ra of all minerals tested on a mass basis, but adsorption to pyrite far exceeds all other minerals when normalized to surface area. In accordance with other studies, we find that pH plays a crucial role in determining the extent of Ra sorption to most mineral surfaces; Ra adsorption to Fe (hydr)oxides and pyrite is extensive at neutral to high pH, yet limited under acidic conditions.

Materials and Methods

Dissolved ^{226}Ra stock in 3% HCl was provided by the MIT Environmental, Health, and Safety office and used for all experiments. A ferrihydrite slurry and goethite powder were prepared using standard methods and added to the experiments.[13] Powdered calcium montmorillonite STX-1b was ordered from the clay minerals society (clays.org), re-equilibrated

with sodium chloride to allow for closer comparisons to previous studies of Ra sorption to Na-montmorillonites, and then cleaned of carbonates using standardized techniques.[14] Pyrite was ordered from Ward's Science (www.wardsci.com), ground using mortar and pestle, passed through sieves to select for 45-250 μm particles, and transferred to an anaerobic glove bag (5% H_2: 95% N_2: < 1 ppm O_2). It was then washed in 6 N HCl overnight to dissolve any oxidized coatings, rinsed with deoxygenated DI water three times to remove residual acid, and dried anaerobically at room temperature. The composition of pyrite, ferrihydrite and goethite was confirmed using XRD, and surface area was measured for all minerals using BET (table S1). Further information about mineral preparation can be found in the supporting information.

Isotherms were conducted using serum vials (200 mL) filled with 100 mL of 10 mM NaCl stock solution, 30 mg of a single mineral (except for the case of pyrite, where 40 mg was used), and 5-270 Bq of ^{226}Ra stock. Experiments using pyrite were performed in an anaerobic glove bag, and all solutions were purged with N_2 prior to placement in the anaerobic chamber. The pH was titrated to 3,5,7 or 9 +/- 0.05 through use of an autotitrator, and the bottle was sealed with a thick butyl stopper. Bottles were shaken for 24 hours to allow sufficient time for sorption equilibrium.[11] A kinetic study of Ra adsorption to montmorillonite confirmed 24 hours is sufficient to achieve equilibrium. pH was readjusted after equilibration if necessary; details on this process are in the supporting information. Acid (HCl) and base (NaOH) volume additions did not exceed 5% of the original solution-slurry volume. Once re-titration and re-equilibration were complete, samples were filtered using 0.22 μm PES filters, which did not sorb significant quantities of Ra. Experimental error was quantified by measuring the standard deviation of triplicates for each data point.

Analytical Techniques. Solutions of Ra were quantified using scintillation counting. Up to 10 mL of sample were mixed with 10 mL of Ultima Gold XR (Perkin Elmer) and sealed for 30 days to allow ^{226}Ra to reach secular equilibrium with its daughter products. The equilibrated samples were then counted using a Beckman Coulter LS 6500 scintillation counter, and the resulting counts were compared to a calibration curve of similarly prepared ^{226}Ra standards to determine solution activities. This was sufficient to determine the extent of sorption and develop isotherms, with the single exception of experiments using ferrihydrite at pH 9, where gamma spectroscopy was used to quantify Ra. Details of the gamma spectroscopy and ^{226}Ra standards are in the supporting information.

Surface Complexation Modeling.

Radium interaction with mineral surfaces was modeled through a double diffuse layer (DDL) surface complexation model implemented in PHREEQC.[15] Reaction formulations developed from spectroscopic measurements and used in previous studies were used to fit experimental data.[11,12] Details for fitting SCMs here along with some alternative modeling strategies are found in the supporting information.

Results and Discussion

Sorption isotherms. All fitted isotherms were linear within the range of activities studied, and isotherm results (normalized by mass) are plotted in figure 1. A K_d value was also calculated by fitting a line to the experimental data (Table S1). Sorption to both iron (hydr)oxides show a strong dependence on pH, with ferrihydrite showing greater sorption across all pH values compared to goethite, and the extent of sorption increasing with increasing pH for both iron (hydr)oxides. Differences in the surface area (table S1) explain some of the variation when

comparing the extent of Ra sorption for goethite and ferrihydrite sorption, with ferrihydrite having nearly twice the surface area of goethite. Accordingly, normalization of sorbed Ra concentrations by mineral surface area (figure 2), as well as a K_{sa}, defined as the K_d normalized by the mineral surface area (m^2/g) (table S1), are used to compare the extent of Ra adsorption between treatments. At circumneutral pH, goethite and ferrihydrite have relatively close K_{sa} values, however at more extreme values (pH = 3 and pH = 9), ferrihydrite demonstrates an appreciably larger extent of sorption compared to goethite. Two studies report isotherm data for Ra sorption to ferrihydrite, and the experimental results presented here match both reported values to within an order of magnitude of the K_d values.[11,16] The K_d found in our study is the largest of the collected data sets, but was also performed at lower background ionic strength (here, 10 mM, others, 100-500 mM) and higher mineral surface area (here, 382.9 m^2/g, others, ~250 m^2/g) , consistent with previous results demonstrating that increased salinity reduces the extent of Ra sorption.[9] One study compared Ra sorption to hematite, ferrihydrite, goethite, and lepidocrocite, finding that ferrihydrite sorbs Ra most extensively.[16] This suggests the sorption isotherm results presented here represent an upper limit for Ra sorption to iron (hdyr)oxides in these conditions.

Reported K_d values for Ra adsorption to goethite (and experimental conditions) vary widely (table S2).[11,16,17] Unlike results obtained for ferrihydrite, we observe a larger extent of Ra sorption at pH 7 and 9, which may be attributed to differences in solution ionic strength and surface area of the synthesized goethite. When normalized by surface area, K_d values are similar in some cases,[11] but are different in others where ionic strength was much higher.[16] Although the goethite synthesized here should more closely match those found in natural settings,[13] other studies used different synthesis methods that often result in lower surface area. The differences

between the results here and in other studies underscore the limitations of using K_d to describe and report solute-solid interactions.

Sorption isotherm results for Ra onto sodium montmorillonite are plotted in figures 1 and 2, the calculated K_d and K_{sa} values listed in table S1. With the exception of ferrihydrite at pH 9, the total extent of sorption to montmorillonite is larger than iron (hydr)oxides over all pH values. Also, a comparatively weaker pH dependence is observed for montmorillonite sorption. This result implies that the dominant mechanism controlling montmorillonite sorption is not complexation with pH dependent surface (edge) functional groups, but rather exchange of Ra with clay interlayer cations. Comparison of the measured sorption K_d values here to earlier studies reveal appreciable differences, with values spanning approximately one order of magnitude (table S2). Those using a high solid-solution ratio (3000-50000 mg/L) resulted in less sorption compared to the sorption results found here, which used only a 300 mg/L solid-solution ratio.[14,18] The CEC of the montmorillonites are similar to that used in this experiment (within 10 meq/100 g clay), and albeit higher here, surface areas are within a factor of three of each other, suggesting interlayer charge is also similar.

Pyrite showed limited sorption of Ra at low pH (3 and 5), but appreciable sorption at higher values, with little difference observed between isotherms performed at pH 7 and 9 (figure 1). The circumneutral and basic K_d values (table S1) for pyrite are comparable to that of goethite at a circumneutral pH. Unexpectedly, calculated surface area normalized sorption isotherms show that pyrite has the largest sorption of all of the minerals considered here (figure 2). There is very little, if any existing data examining the sorption of Ra to any reduced iron solid. A previous study demonstrated that strontium (Sr), which possesses analogous geochemical characteristics as Ra, did not sorb extensively to pyrite[19], but little other data exists regarding

group II cation sorption to unoxidized pyrite surfaces. In contrast, a variety of experimental and spectroscopic techniques to study redox active metal ions sorption to the pyrite surface, which often includes redox reactions between the metal ion and pyrite surface groups.[19–24] The results of these studies imply that redox active metal ions or trace quantities of dissolved oxygen in solutions with Ra may alter the pyrite surface, consequentially diminishing or enhancing Ra sorption. However, we find no evidence of (oxic) pyrite alteration in our experimentation, and exceedingly low Ra concentrations (0.06-31 nmoles per experiment) preclude other methods for examining the coordination environment of adsorbed Ra.

Surface Complexation Modeling.

Concentrations of Ra used here are below the analytical detection limits of most techniques (e.g. X-ray spectroscopy) used to validate the bonding environment of Ra to solids. Hence, SCM developed for Ra adsorption is compared with other studies that combine SCM with spectroscopic measurements used to constrain surface reactions of other group II elements. In a previous study, X-ray absorption spectroscopy was used to examine Sr binding with the surface of iron (hydr)oxides, revealing it forms outer sphere complexes.[25] A separate study used SCM informed by x-ray spectroscopy to constrain group II element sorption to iron (hydr)oxides, and predicted tetradentate coordination of Ra with iron (hydr)oxide surface sites.[12,26] Accordingly, Ra adsorption to ferrihydrite and goethite was simulated here by using two tetradentate reactions with a single site—fitted parameters closely match experimental data (figure 3). This approach was also successfully used by Sajih et al (2014) for simulating Ra adsorption to ferrihydrite and goethite, abeit at substantially higher levels of Ra. The fitted reactions and constants (table 1) show that ferrihydrite and goethite have roughly similar reaction constants, but ferrihydrite has more sites, explaining the greater observed sorption extent. While

Commented [Office1]: Expand this sentence

the reaction constants found here are only a few log units larger than other studies' goethite results, the constants for ferrihydrite sorption reactions here are nearly 20 orders of magnitude smaller.[11,12] Although this disparity is quite large, it is known that the structural properties (crystallinity, crystal unit size, water content) of ferrihydrite may vary substantially according to the method used for synthesis, which may account for some of the variance.[27]

To test the importance of (inferred) tetradentate Ra coordination with mineral surfaces, simulations were performed using simplified reactions (table 3SI), and yielded poor fits to the data. This eliminates the validity of a "simplified" reaction scheme for modeling Ra adsorption to Fe (hydr)oxides, and favors the use of the tetradentate model. However, despite providing good fits to experimental data, thermodynamic constants found through modeling reactions using Ra-tetradentate coordination do not closely match the constants predicted by a previous study.[12] A problem that arises when comparing SCM results is that multiple reaction formulations can satisfy the constraints developed by spectroscopic observations, without a clear indication as to which is a more accurate description of sorption or if those constraints are applicable to other elements with similar chemistry.[12] These complications, and variations in experimental methodology for SCM, underscore the ongoing need to make measurements of Ra sorption to mineral surfaces using the same (or similar) analytical techniques used for other group II elements.[28]

Surface complexation modeling of Ra adsorption to sodium montmorillonite was fit using two surface sites and an exchange reaction where Ra displaces sodium in the inner layer of the clay, following previous SCM studies of metal sorption to montmorillonites (Table 1).[29] Fits using this model were visually good (Figure 3), and the exchange reaction accounts for extensive Ra sorption over all pH values. A previous study used a similar suite of reactions to describe Ba

adsorption to Na-montmorillonite, and X-ray absorption spectroscopy confirmed the formation of both inner sphere and outer sphere complexes on the montmorillonite surface corresponding with the need for both an exchange reaction and surface site reactions in the SCM.[30] The number of fitted sites in this model were significantly lower than reported in the literature, with literature values producing poor fits. The presence of exchange in these models account for the significant extent of sorption at acidic pHs, and the fitted surface complexation constants in either model also suggest that Ra binds more extensively with the clay surface than either of the iron (hydr)oxides.

Although SCM has not been extensively used to examine group II cation adsorption with montmorillonites, there is a broad base of literature examining the selectivity of exchange and surface reactions with other metals.[31] Previously calculated metal exchange reactions with sodium montmorillonite cations show a range of values from 0.7 to 398, compared to 1.41 found here for Ra exchange. This suggests that Ra could easily be displaced by other metals in solution. Since a large fraction of the observed Ra adsorption is associated with the exchange reaction (i.e. sorption observed at low pH), this competition from other metals will likely play a large role in controlling Ra sorption to montmorillonite and other clays with a cation-exchangeable interlayer. In contrast, Ra had a relatively large surface complex reaction constants (0 and 7.5) compared to those found for other potentially hazardous metals (-20 to 2).[29,32] This suggests that less competition for the protonated surface sites will occur in the presence of other metals, though it is unclear how ion exchange will control the ultimate fate of Ra in high salinity environments with many competing cations, particularly divalent cations with high selectivity.

Lastly, SCM of Ra adsorption to pyrite was performed using surficial S as the adsorption site (Table 1),[20] based on a previous SCM that modeled Sr sorption to pyrite.[19] Model fits of Ra

sorption capture the observed data points, though not as well as for Ra adsorption to montmorillonite or iron (hydr)oxides (Figure 3). The fitted reaction constant is also the lowest of all of the fitted reaction constants found here by multiple orders of magnitude. This confirms the results when comparing K_d values in between minerals, yet is contradicted by the K_{sa} results that showed that pyrite had the largest amount of surface area normalized sorption. Increases in the total number of surface sites in the SCM were not able to fit the experimental data accurately, which suggests that this formulation of the SCM is inaccurate with respect to the actual pyrite-Ra surface complexes. Further analytical investigation using surface-sensitive measurements may elucidate mechanisms of Ra sorption.

Implications for radium mobility in soils and aquifers

Experimental and SCM results highlight both preferential sorption of Ra to different mineral phases present in soils and natural aquifers, as well as the dynamic adsorption equilibria of Ra when (bio)geochemical conditions are altered, including changes in pH and mineralogy. Radium adsorbed extensively to every mineral examined, albeit maximum adsorption varied according to pH and nature of the exchange site(s) on the mineral surface. Hence, using literature-reported K_d values for predicting Ra mobility in natural systems may be erroneous if solution conditions and possible sorbing phases are not considered. In light of this, groundwater model predictions and estimations employing the use of Ra as a tracer may improve by measuring total Ra (and in some scenarios, Ra isotopes) associated with dominant subsurface minerals, and incorporating adsorption processes into simplistic mixing models.

References

(1) Zhang, T.; Gregory, K.; Hammack, R. W.; Vidic, R. D. *Environ. Sci. Technol.* **2014**, *48* (8), 4596–4603.

(2) Jones, A. P. *Atmos. Environ.* **1999**, *33* (28), 4535–4564.

(3) Lu, N.; Mason, C. F. V. *Appl. Geochemistry* **2001**, *16* (14), 1653–1662.

(4) Szabo, Z.; dePaul, V. T.; Fischer, J. M.; Kraemer, T. F.; Jacobsen, E. *Appl. Geochemistry* **2012**, *27* (3), 729–752.

(5) Barbot, E.; Vidic, N. S.; Gregory, K. B.; Vidic, R. D. *Environ. Sci. Technol.* **2013**, *47* (6), 2562–2569.

(6) Vengosh, A.; Hirschfeld, D.; Vinson, D.; Dwyer, G.; Raanan, H.; Rimawi, O.; Al-zoubi, A.; Akkawi, E.; Marie, A.; Haquin, G.; Zaarur, S.; Ganor, J. *Environ. Sci. Technol.* **2009**, *43*, 1769–1775.

(7) Lauer, N.; Vengosh, A. *Environ. Sci. Technol. Lett.* **2016**, acs.estlett.6b00118.

(8) Fesenko, S.; Carvalho, F.; Martin, P.; Moore, W. S.; Yankovich, T. *Radium in the Environment*; 2014.

(9) Gonneea, M. E.; Morris, P. J.; Dulaiova, H.; Charette, M. a. *Mar. Chem.* **2008**, *109* (3–4), 250–267.

(10) Grivé, M.; Duro, L.; Colàs, E.; Giffaut, E. *Appl. Geochemistry* **2015**, *55*, 85–94.

(11) Sajih, M.; Bryan, N. D. D.; Livens, F. R. R.; Vaughan, D. J. J.; Descostes, M.; Phrommavanh, V.; Nos, J.; Morris, K. *Geochim. Cosmochim. Acta* **2014**, *146*, 150–163.

(12) Sverjensky, D. A. *Geochim. Cosmochim. Acta* **2006**, *70* (10), 2427–2453.

(13) Schwertmann, U.; Cornell, R. *Iron Oxides in the Laboratary*; Wiley-VCH Verlag GmbH: Weinheim, Germany, 2000.

(14) Tamamura, S.; Takada, T.; Tomita, J.; Nagao, S.; Fukushi, K.; Yamamoto, M. *J. Radioanal. Nucl. Chem.* **2013**, *299* (1), 569–575.

(15) Parkhurst, D. L.; Appela, C. A. J. *Description of Input and Examples for PHREEQC Version 3 — A Computer Program for Speciation , Batch-Reaction , One-Dimensional Transport , and Inverse Geochemical Calculations Chapter 43 of*; 2013.

(16) Beck, A. J.; Cochran, M. a. *Mar. Chem.* **2013**, *156*, 38–48.

(17) Nirdosh, I.; Trembley, W.; Johnson, C. *Hydrometallurgy* **1990**, *24* (2), 237–248.

(18) Ames, L. L. *Clays Clay Miner.* **1983**, *31* (5), 321–334.

(19) Naveau, A.; Monteil-Rivera, F.; Dumonceau, J.; Catalette, H.; Simoni, E. *J. Colloid Interface Sci.* **2006**, *293* (1), 27–35.

(20) Murphy, R.; Strongin, D. *Surf. Sci. Rep.* **2009**, *64* (1), 1–45.

(21) Kornicker, W. A.; Morse, J. W. *Geochim. Cosmochim. Acta* **1991**, *55* (8), 2159–2171.

(22) Wersin, P.; Hochella, M. F.; Persson, P.; Redden, G.; Leckie, J. O.; Harris, D. W. *Geochim. Cosmochim. Acta* **1994**, *58* (13), 2829–2843.

(23) Naveau, A.; Monteil-Rivera, F.; Guillon, E.; Dumonceau, J. *Environ. Sci. Technol.* **2007**, *41* (15), 5376–5382.

(24) Das, D. K.; Pathak, P. N.; Kumar, S.; Manchanda, V. K. *J. Radioanal. Nucl. Chem.* **2009**, *281* (3), 449–455.

(25) Sahai, N.; Carroll, S. A.; Roberts, S.; O'Day, P. A. *J. Colloid Interface Sci.* **2000**, *222* (2), 198–212.

(26) Fenter, P.; Cheng, L.; Rihs, S.; Machesky, M. L.; Bedzyk, M. J.; Sturchio, N. C. *J. Colloid Interface Sci.* **2000**, *225*, 154–165.

(27) Michel, F. M.; Ehm, L.; Antao, S. M.; Lee, P. L.; Chupas, P. J.; Liu, G.; Strongin, D. R.; Schoonen, M. a a; Phillips, B. L.; Parise, J. B. *Science* **2007**, *316* (5832), 1726–1729.

(28) Duster, T. A. *Environ. Sci. Technol.* **2016**, *50* (14), 7274–7275.

(29) Bradbury, M. H.; Baeyens, B. *Geochim. Cosmochim. Acta* **2005**, *69* (4), 875–892.

(30) Zhang, P. C.; Brady, P. V.; Arthur, S. E.; Zhou, W. Q.; Sawyer, D.; Hesterberg, D. A. *Colloids Surfaces A Physicochem. Eng. Asp.* **2001**, *190* (3), 239–249.

(31) Bradbury, M. H.; Baeyens, B.; Geckeis, H.; Rabung, T. *Geochim. Cosmochim. Acta* **2005**, *69* (23), 5403–5412.

(32) Gorgeon, L. Contribution à la Modélisation Physico-Chimique de la Retention de Radioéléments à Vie Longue par des Matériaux Argileux, Universite Paris, 1994.

330

331 **Table 1:** Reactions and Constants used in Surface Complexation Modeling

Reactions	Sites (mol/g)	log K	Source
Ferrihydrite	1.75E-3		[11]
$\equiv FhyOH + H^+ \rightleftarrows \equiv FhyOH_2^+$		7.92	[11]
$\equiv FhyOH \rightleftarrows \equiv FhyO^- + H^+$		-8.93	[11]
$4\equiv FhyOH + Ra^{2+} \rightleftarrows \equiv (FhyOH)_3FhyORa^+ + H^+$		-1.4	Fitting
$4\equiv FhyOH + Ra^{2+} + 2H^+ \rightleftarrows \equiv (FhyOH_2)_2(FhyOH)_2Ra^{4+}$		0	Fitting
Goethite	6.4E-5		[12]
$\equiv GoeOH + H^+ \rightleftarrows \equiv GoeOH_2^+$		4.8	[12]
$\equiv GoeOH \rightleftarrows \equiv GoeO^- + H^+$		-10.4	[12]
$4\equiv GoeOH + Ra^{2+} \rightleftarrows \equiv (GoeOH)_3GoeORa^+$		-2.9	Fitting
$4\equiv GoeOH + Ra^{2+} \rightleftarrows \equiv (GoeOH)_4Ra^{2+}$		4.6	Fitting
Sodium Montmorillonite			
$2 \equiv Clay\text{-}Na + Ra^{2+} \rightleftarrows \equiv Clay_2\text{-}Ra + 2\ Na^+$	Exch: 8.43E-4	0.15	Fitting
$\equiv Clay_AOH + H^+ \rightleftarrows Clay_AOH_2^+$	Site A: 2E-7	4.5	[31]
$\equiv Clay_AOH \rightleftarrows \equiv Clay_A^- + H^+$		-7.9	[31]
$\equiv Clay_BOH + H^+ \rightleftarrows Clay_BOH_2^+$	Site B: 6.33E-7	4.5	[31]
$\equiv Clay_BOH \rightleftarrows \equiv Clay_B^- + H^+$		-7.9	[31]
$\equiv Clay_AOH + Ra^{2+} \rightleftarrows \equiv Clay_AORa^+ + H^+$		0	Fitting
$\equiv Clay_BOH + Ra^{2+} \rightleftarrows \equiv Clay_BOHRa^{2+}$		7.5	Fitting
Pyrite	2.23E-5		[19]
$\equiv PyrSH \rightleftarrows \equiv PyrS\text{-} + H^+$		6.45	[19]
$\equiv PyrS^- + Ra^{2+} \rightleftarrows \equiv PyrSRa^+$		-10.5	Fitting

332

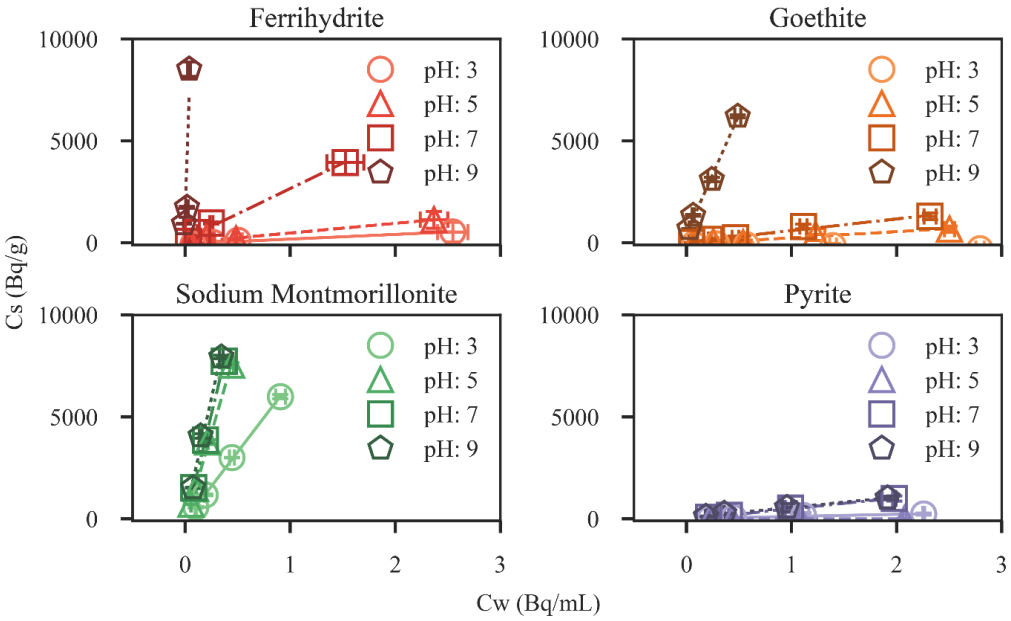

Figure 1: Isotherm results for the studied minerals. Error bars represent the standard deviation of the triplicate measurement. Fit lines' slope matches the measured K_d values reported in Table S1.

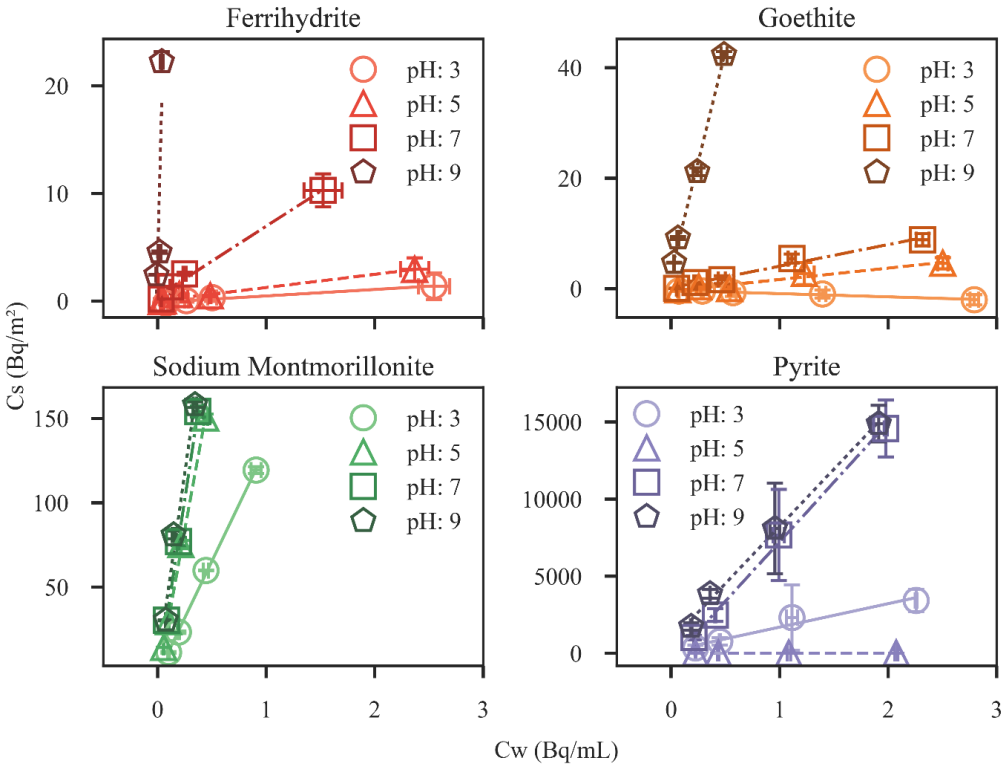

Figure 2: Isotherm results for the studied minerals, normalized by mineral surface area. Error bars represent the standard deviation of the triplicate experiment, and fit lines the corresponding K_{sa} in Table S1.

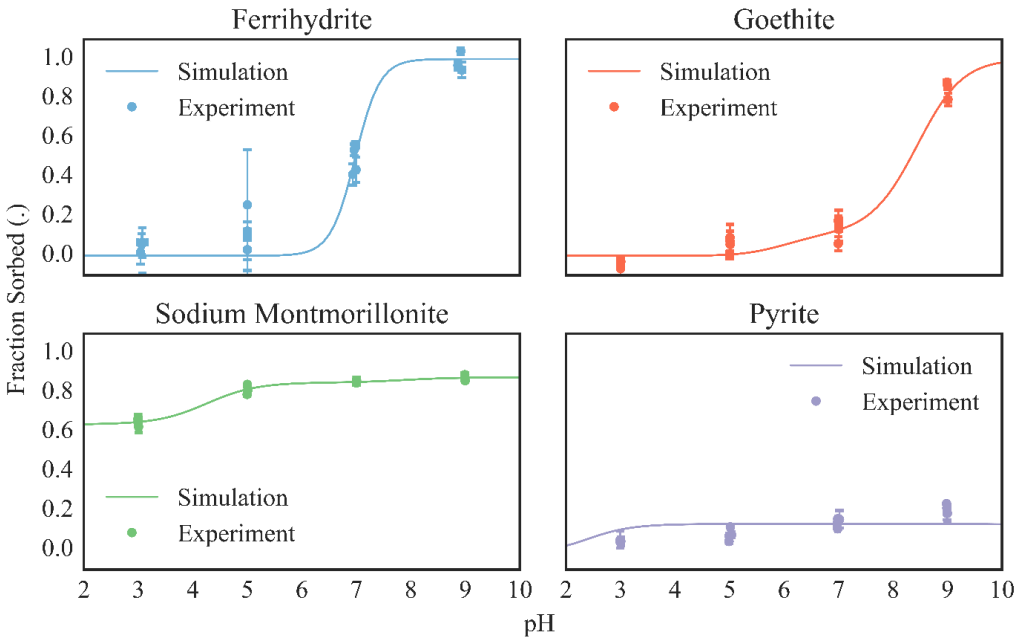

340

341 **Figure 3:** SCM results (lines) compared against experimental results (points) for the studied

342 minerals. Error bars on data points represent standard deviation of triplicate experimental

343 measurements.